OPEN ACCESS
Fractals, Vol. 29, No. 5 (2021) 2140015 (11 pages)

DOI: 10.1142/S0218348X21400156

World Scientific
www.worldscientific.com

A FRACTAL FRACTIONAL MODEL FOR CERVICAL CANCER DUE TO HUMAN PAPILLOMAVIRUS INFECTION

A. AKGÜL,[*,††] N. AHMED,[†] A. RAZA,[‡] Z. IQBAL,[†] M. RAFIQ,[§]
M. A. REHMAN[†] and D. BALEANU[¶,‖,**]

[*]*Department of Mathematics, Art and Science Faculty*
Siirt University, TR-56100 Siirt, Turkey

[†]*Department of Mathematics and Statistics*
The University of Lahore, Lahore, Pakistan

[‡]*Department of Mathematics*
National College of Business Administration and Economics
Lahore, Pakistan

[§]*Department of Mathematics, Faculty of Sciences*
University of Central Punjab, Lahore, Pakistan

[¶]*Department of Mathematics, Cankaya University*
06530 Balgat, Ankara, Turkey

[‖]*Institute of Space Sciences, R76900 Magurele-Bucharest, Romania*

[**]*Department of Medical Research, China Medical University*
Taichung 40402, Taiwan

[††]*aliakgul00727@gmail.com*

Received July 19, 2020
Accepted October 26, 2020
Published March 4, 2021

[††]Corresponding author.

Abstract

In this paper, we have investigated women's malignant disease, cervical cancer, by constructing the compartmental model. An extended fractal–fractional model is used to study the disease dynamics. The points of equilibria are computed analytically and verified by numerical simulations. The key role of R_0 in describing the stability of the model is presented. The sensitivity analysis of R_0 for deciding the role of certain parameters altering the disease dynamics is carried out. The numerical simulations of the proposed numerical technique are demonstrated to test the claimed facts.

Keywords: Cancer Model; Numerical Simulations; Disease.

1. INTRODUCTION

The cervix is a cylinder-shaped tissue that connects the women vagina and uterus with each other. Cervical cancer is a special type of cancer which comes about by the cervix. It is due to the growth of those cells which have the ability to attack and spread into other parts of the body. In the initial stages, no symptoms arise. But, later on, main symptoms in victims such as abnormal vaginal bleeding, pelvic pain or pain during sexual intercourse may be noted. There are more than 90% cases of cervical cancer which are due to HPV (human papillomavirus), while other factors causing this disease are smoking, low immunity, pills for birth control and sex at very early age. It is grown from precancerous cells in 10 to 20 years. It is a highly risky disease, which causes four tiers of death rates in women. Due to this disease, about 8% of cancers develop in women. In underdeveloped countries, this cancer is one of the most common causes of death. On the other hand, in developed countries, about 70% of cervical cancer cases result in 90% mortality rate. It is usually diagnosed by biopsy technique. The most common techniques use for treatment are surgery, chemotherapy, radiation therapy and immunotherapy.[1] In 2019, Chakraborty *et al.*[2] furnished the control-based comparative study of HPV on cervical cancer with several functional responses. In 2014, Pongsumpun[3] investigated the deterministic analysis of cervical cancer due to human papillomavirus infection. Taylor *et al.*[4] studied the Markov properties in modeling of cervical cancer with computational methods. Khattak *et al.*[5] discussed the active role of therapies to overcome the cervical cancer by using mathematical techniques. Bitok *et al.*[6] purposed mathematical model for cervical cancer in Kenya. They pointed out two stages in women as diagnosed and undiagnosed. Also, they described the population of women in two ways. In 2012, Lee *et al.*[7] developed the modeling of HPV and its impact on cervical cancer in the United states. They presented a compartmental mathematical model for the cycle of HPV. In 2018, Peng *et al.*[8] found the age-structured model for cervical cancer in Texas, United states, in which they introduced more compartments of population and presented a model, with a large number of equations. In 2019, Sado[9] developed a model of cervical cancer with HPV transmission in which he shared an idea of cervical cancer by HPV with and without vaccination strategy.[9] In 2018, Asih *et al.*[10] studied cell dynamics of cervical cancer in human population and its control strategies. In 2015, Lestari *et al.*[11] presented the model of HPV by using gene therapy with the fashion of Lotka–Volterra model. In 2015, Mazlan *et al.*[12] found the stochastic model of cervical cancer with delay effect by introducing the random perturbation like uncontrolled environmental factors and included deceleration factor in growth rate. In 2006, Barnabas *et al.*[13] presented the epidemiology of HPV and cervical cancer in Finland and discussed the potential impact of vaccination. In 2008, Goldie *et al.*[14] described the model of cervical cancer prevention in the Asia Pacific region in which they estimated the cervical cancer cases causing deaths and disability. In 2018, Peprah *et al.*[15] performed the spatiotemporal analysis of cervical cancer with HPV in Maryland. In 2017, Xia *et al.*[16] carried out the geographical analysis of mortality rate due to cervical cancer by considering spatio-temporal study. In 2006, Dasbach *et al.*[17] narrated three types of models of cervical cancer in which they have predicted cost effectiveness of vaccination plans for overcoming the disease. In 2017, Zhao *et al.*[18] presented a model of cervical cancer

by using spatio-temporal mapping in Thailand. In 2008, Goldie *et al.*[19] investigated the fatality rate, function of vaccination and disability caused by cervical cancer in Latin America with a mathematical model. In 2015, Herrmann *et al.*[20] studied the cervical cancer in which they considered the mortality rate due to breast, ovarian, cervical and uterine cancer in Switzerland. Some best fit models can be obtained by using the new fractional operators presented in Refs. 21–33.

2. PRELIMINARIES

Definition 1. We assume that $u(t)$ is continuous in (a, b) and differentiable on (a, b) with order θ. Then, the fractal-fractional derivative of u of order γ in Riemann–Liouville sense with the generalized Mittag–Leffler kernel is presented by Ref. 24 as

$$
\begin{aligned}
{}^{\mathrm{FFM}}_{a}D_t^{\gamma,\theta}u(t) &= \frac{\mathrm{AB}(\gamma)}{1-\gamma}\frac{d}{dt^{\theta}}\int_a^t u(y)E_{\gamma} \\
&\quad \times\left(\frac{-\gamma}{1-\gamma}(t-y)^{\gamma}\right)dy, \\
&\quad 0<\gamma, \quad \theta \le 1, \qquad (1)
\end{aligned}
$$

where $\mathrm{AB}(\gamma) = 1-\gamma+\frac{\gamma}{\Gamma(\gamma)}$.

Definition 2. Assume that $u(t)$ is continuous in (a, b). Then the fractal-fractional integral of u with order γ is given by Ref. 24 as

$$
\begin{aligned}
{}^{\mathrm{FFM}}_{0}I_t^{\gamma,\theta}u(t) &= \frac{\theta\gamma}{\mathrm{AB}(\gamma)\Gamma(\gamma)}\int_0^t y^{\theta-1}u(y) \\
&\quad \times (t-y)^{\gamma-1}dy \\
&\quad + \frac{\theta(1-\gamma)t^{\theta-1}}{\mathrm{AB}(\gamma)}u(t). \qquad (2)
\end{aligned}
$$

3. DISCRETIZATION AND STABILITY WITH THE GENERALIZED MITTAG–LEFFLER KERNEL

We consider the following problem:

$$S_p' = \mu_h - (P_v I_{\mathrm{HPV}} + \mu_h)S_p, \qquad (3)$$

$$I_{\mathrm{HPV}}' = (P_v S_p - P_c - \mu_h)I_{\mathrm{HPV}}, \qquad (4)$$

$$I_{cc}' = P_c I_{\mathrm{HPV}} - \mu_h I_{cc}. \qquad (5)$$

We replace the classical derivatives of the above system with the fractal fractional derivatives and obtain

$$
\begin{aligned}
{}^{\mathrm{FFM}}_{a}D_t^{\gamma,\theta}S_p &= \mu_h - (P_v I_{\mathrm{HPV}} + \mu_h)S_p, \qquad (6)\\
{}^{\mathrm{FFM}}_{a}D_t^{\gamma,\theta}I_{\mathrm{HPV}} &= (P_v S_p - P_c - \mu_h)I_{\mathrm{HPV}}, \qquad (7)\\
{}^{\mathrm{FFM}}_{a}D_t^{\gamma,\theta}I_{cc} &= P_c I_{\mathrm{HPV}} - \mu_h I_{cc}. \qquad (8)
\end{aligned}
$$

Then, we get

$$
\begin{aligned}
&\frac{\mathrm{AB}(\alpha)}{1-\alpha}\frac{d}{dt}\int_0^t S_p(\tau)E_{\alpha} \\
&\quad \times\left(\frac{-\alpha}{1-\alpha}(t-\tau)^{\alpha}\right)d\tau \\
&= \beta t^{\beta-1}\big(\mu_h - (P_v I_{\mathrm{HPV}} + \mu_h)S_p\big), \qquad (9)\\
&\frac{\mathrm{AB}(\alpha)}{1-\alpha}\frac{d}{dt}\int_0^t I_{\mathrm{HPV}}(\tau)E_{\alpha} \\
&\quad \times\left(\frac{-\alpha}{1-\alpha}(t-\tau)^{\alpha}\right)d\tau \\
&= \beta t^{\beta-1}(P_v S_p - P_c - \mu_h)I_{\mathrm{HPV}}, \qquad (10)\\
&\frac{\mathrm{AB}(\alpha)}{1-\alpha}\frac{d}{dt}\int_0^t I_{cc}(\tau)E_{\alpha} \\
&\quad \times\left(\frac{-\alpha}{1-\alpha}(t-\tau)^{\alpha}\right)d\tau \\
&= \beta t^{\beta-1}\big(P_c I_{\mathrm{HPV}} - \mu_h I_{cc}\big). \qquad (11)
\end{aligned}
$$

For simplicity, we define

$$
\begin{aligned}
&F(t, S_p, I_{\mathrm{HPV}}, I_{cc}) \\
&\quad = \beta t^{\beta-1}(\mu_h - (P_v I_{\mathrm{HPV}} + \mu_h)S_p), \qquad (12)\\
&G(t, S_p, I_{\mathrm{HPV}}, I_{cc}) \\
&\quad = \beta t^{\beta-1}(P_v S_p - P_c - \mu_h)I_{\mathrm{HPV}}, \qquad (13)\\
&H(t, S_p, I_{\mathrm{HPV}}, I_{cc}) \\
&\quad = \beta t^{\beta-1}(P_c I_{\mathrm{HPV}} - \mu_h I_{cc}). \qquad (14)
\end{aligned}
$$

Then, we will get

$$
\begin{aligned}
&\frac{\mathrm{AB}(\alpha)}{1-\alpha}\frac{d}{dt}\int_0^t S_p(\tau)E_{\alpha} \\
&\quad \times\left(\frac{-\alpha}{1-\alpha}(t-\tau)^{\alpha}\right)d\tau \\
&\quad = F(t, S_p, I_{\mathrm{HPV}}, I_{cc}), \qquad (15)
\end{aligned}
$$

$$\frac{\mathrm{AB}(\alpha)}{1-\alpha}\frac{d}{dt}\int_0^t I_{\mathrm{HPV}}(\tau)E_\alpha \times\left(\frac{-\alpha}{1-\alpha}(t-\tau)^\alpha\right)d\tau = G(t,S_p,I_{\mathrm{HPV}},I_{cc}), \tag{16}$$

$$\frac{\mathrm{AB}(\alpha)}{1-\alpha}\frac{d}{dt}\int_0^t I_{cc}(\tau)E_\alpha \times\left(\frac{-\alpha}{1-\alpha}(t-\tau)^\alpha\right)d\tau = H(t,S_p,I_{\mathrm{HPV}},I_{cc}). \tag{17}$$

By applying the AB integral, we will capture the following expressions:

$$S_p(t)-S_p(0) = \frac{1-\alpha}{\mathrm{AB}(\alpha)}F(t,S_p,I_{\mathrm{HPV}},I_{cc}) + \frac{\alpha}{\mathrm{AB}(\alpha)\Gamma(\alpha)}\int_0^t (t-\tau)^{\alpha-1} \times F(\tau,S_p,I_{\mathrm{HPV}},I_{cc})d\tau,$$

$$I_{\mathrm{HPV}}(t)-I_{\mathrm{HPV}}(0) = \frac{1-\alpha}{\mathrm{AB}(\alpha)}G(t,S_p,I_{\mathrm{HPV}},I_{cc}) + \frac{\alpha}{\mathrm{AB}(\alpha)\Gamma(\alpha)}\int_0^t (t-\tau)^{\alpha-1} \times G(\tau,S_p,I_{\mathrm{HPV}},I_{cc})d\tau,$$

$$I_{cc}(t)-I_{cc}(0) = \frac{1-\alpha}{\mathrm{AB}(\alpha)}H(t,S_p,I_{\mathrm{HPV}},I_{cc}) + \frac{\alpha}{\mathrm{AB}(\alpha)\Gamma(\alpha)}\int_0^t (t-\tau)^{\alpha-1}H \times(\tau,S_p,I_{\mathrm{HPV}},I_{cc})d\tau.$$

Now, we discretize these equations at t_{n+1} as

$$S_p^{n+1} = S_p^0 + \frac{1-\alpha}{\mathrm{AB}(\alpha)} \times F(t_{n+1},S_p^n,I_{\mathrm{HPV}}^n,I_{cc}^n) + \frac{\alpha}{\mathrm{AB}(\alpha)\Gamma(\alpha)} \times \int_0^{t_{n+1}}(t_{n+1}-\tau)^{\alpha-1} \times F(\tau,S_p,I_{\mathrm{HPV}},I_{cc})d\tau,$$

$$I_{\mathrm{HPV}}^{n+1} = I_{\mathrm{HPV}}^0 + \frac{1-\alpha}{\mathrm{AB}(\alpha)} \times G(t_{n+1},S_p^n,I_{\mathrm{HPV}}^n,I_{cc}^n) + \frac{\alpha}{\mathrm{AB}(\alpha)\Gamma(\alpha)} \times \int_0^{t_{n+1}}(t_{n+1}-\tau)^{\alpha-1} \times G(\tau,S_p,I_{\mathrm{HPV}},I_{cc})d\tau,$$

$$I_{cc}^{n+1} = I_{cc}^0 + \frac{1-\alpha}{\mathrm{AB}(\alpha)} \times H(t_{n+1},S_p,I_{\mathrm{HPV}},I_{cc}) + \frac{\alpha}{\mathrm{AB}(\alpha)\Gamma(\alpha)}\int_0^{t_{n+1}}(t-\tau)^{\alpha-1} \times H(\tau,S_p,I_{\mathrm{HPV}},I_{cc})d\tau.$$

Then, we obtain

$$S_p^{n+1} = S_p^0 + \frac{1-\alpha}{\mathrm{AB}(\alpha)} \times F(t_{n+1},S_p^n,I_{\mathrm{HPV}}^n,I_{cc}^n) + \frac{\alpha}{\mathrm{AB}(\alpha)} \times \sum_{j=0}^{n}\left[\frac{h^\alpha F(t_j,S_p^n,I_{\mathrm{HPV}}^n,I_{cc}^n)}{\Gamma(\alpha+2)} \times((n+1-j)^\alpha(n-j+2+\alpha) - (n-j)^\alpha(n-j+2+2\alpha))\right] - \frac{\alpha}{\mathrm{AB}(\alpha)} \times \sum_{j=0}^{n}\left[\frac{h^\alpha F(t_{j-1},S_p^{n-1},I_{\mathrm{HPV}}^{n-1},I_{cc}^{n-1})}{\Gamma(\alpha+2)} \times((n+1-j)^{\alpha+1}-(n-j)^\alpha \times(n-j+1+\alpha))\right],$$

$$I_{\mathrm{HPV}}^{n+1} = I_{\mathrm{HPV}}^0 + \frac{1-\alpha}{\mathrm{AB}(\alpha)} \times G(t_{n+1},S_p^n,I_{\mathrm{HPV}}^n,I_{cc}^n) + \frac{\alpha}{\mathrm{AB}(\alpha)} \times \sum_{j=0}^{n}\left[\frac{h^\alpha G(t_j,S_p^n,I_{\mathrm{HPV}}^n,I_{cc}^n)}{\Gamma(\alpha+2)} \times((n+1-j)^\alpha(n-j+2+\alpha) - (n-j)^\alpha(n-j+2+2\alpha))\right] - \frac{\alpha}{\mathrm{AB}(\alpha)}$$

$$\times \sum_{j=0}^{n} \left[\frac{h^{\alpha} G(t_{j-1}, S_p^{n-1}, I_{\text{HPV}}^{n-1}, I_{cc}^{n-1})}{\Gamma(\alpha+2)} \times ((n+1-j)^{\alpha+1} - (n-j)^{\alpha} \times (n-j+1+\alpha)) \right],$$

$$I_{cc}^{n+1} = I_{cc}^{0} + \frac{1-\alpha}{\text{AB}(\alpha)} \times H(t_{n+1}, S_p^n, I_{\text{HPV}}^n, I_{cc}^n) + \frac{\alpha}{\text{AB}(\alpha)} \times \sum_{j=0}^{n} \left[\frac{h^{\alpha} H(t_j, S_p^n, I_{\text{HPV}}^n, I_{cc}^n)}{\Gamma(\alpha+2)} \times ((n+1-j)^{\alpha}(n-j+2+\alpha) - (n-j)^{\alpha}(n-j+2+2\alpha)) \right] - \frac{\alpha}{\text{AB}(\alpha)} \times \sum_{j=0}^{n} \left[\frac{h^{\alpha} H(t_{j-1}, S_p^{n-1}, I_{\text{HPV}}^{n-1}, I_{cc}^{n-1})}{\Gamma(\alpha+2)} \times ((n+1-j)^{\alpha+1} - (n-j)^{\alpha} \times (n-j+1+\alpha)) \right]$$

by the method used in Ref. 25.

4. EQUILIBRIA

We obtain the equilibria of the fractal fractional model as

$$ {}^{\text{FFM}}_{a}D_t^{\gamma,\theta} S_p = 0, \quad {}^{\text{FFM}}_{a}D_t^{\gamma,\theta} I_{\text{HPV}} = 0, \quad {}^{\text{FFM}}_{a}D_t^{\gamma,\theta} I_{cc} = 0. \tag{18}$$

Then, we have

$$\mu_h - (P_v I_{\text{HPV}} + \mu_h) S_p = 0, \tag{19}$$

$$(P_v S_p - P_c - \mu_h) I_{\text{HPV}} = 0, \tag{20}$$

$$P_c I_{\text{HPV}} - \mu_h I_{cc} = 0. \tag{21}$$

After simplification, we will get

$$S_p = 1, \quad I_{\text{HPV}} = 0, \quad I_{cc} = 0. \tag{22}$$

We obtain two types of equilibria of the model. We acquire the cancer-free equilibrium (CFE) as

$$D = (S_p, I_{\text{HPV}}, I_{cc} = (1, 0, 0)). \tag{23}$$

We construct the cervical cancer endemic equilibrium (CEE) as

$$E = (S_p, I_{\text{HPV}}, I_{cc}), \tag{24}$$

where

$$\begin{aligned} S_p &= \frac{P_c + \mu_h}{P_v}, \\ I_{\text{HPV}} &= \mu_h \frac{P_v - P_c - \mu_h}{P_v(P_c + \mu_h)}, \\ I_{cc} &= P_c \frac{P_v - P_c - \mu_h}{P_v(P_c + \mu_h)}, \\ R_0 &= \frac{P_v}{P_c + \mu_h}. \end{aligned} \tag{25}$$

Note that R_0 is cervical cancer generation number. The cervical cancer generation number has an imperative role in learning of the cervical cancer subtleties.

5. LOCAL STABILITY

The jacobean of the model is calculated as follows:

$$j = \begin{bmatrix} -P_v I_{\text{HPV}} - \mu_h & -P_v S_p & 0 \\ P_v I_{\text{HPV}} & P_v S_p - P_c - \mu_h & 0 \\ 0 & P_c & -\mu_h \end{bmatrix}. \tag{26}$$

Theorem 3. *The cancer-free equilibrium $E_o = (1, 0, 0)$ of the model is locally asymptotically stable if $R_0 < 1$ and unstable if $R_0 > 1$.*

Proof. The cancer-free equilibrium $E_o = (1, 0, 0)$ is locally asymptotically stable (LAS) if all the eigenvalues $\lambda_i, i = 1, 2, 3$, satisfy $\lambda_i < 0$ and $|\arg(\lambda_i)| > \frac{\alpha\pi}{2}$. We present the Jacobean matrix at $E_o = (1, 0, 0)$ for the eigen values as

$$\begin{aligned} &|J(E_0) - \lambda I| \\ &= \begin{vmatrix} -\mu_h - \lambda & -P_v & 0 \\ 0 & P_v - P_c - \mu_h - \lambda & 0 \\ 0 & P_c & -\mu_h - \lambda \end{vmatrix} \\ &= 0. \end{aligned} \tag{27}$$

The eigen values $\lambda_1 = -\mu_h < 0$ and $\lambda_3 = -\mu_h < 0$ are same. $\lambda_2 = P_v - P_c - \mu_h < 0$, if $R_o = \frac{P_v}{(P_c + \mu_h)} < 1$. Since all eigen values are negative therefore, the cancer-free equilibrium E_o is locally asymptotically stable. If $R_0 > 1$, that is $\frac{P_v}{(P_c + \mu_h)} > 1$, $P_v > P_c + \mu_h - (P_c + \mu_h) + P_v > 0$. Then $\lambda_2 > 0$. Hence, E_o is unstable. □

Theorem 4. *The cancer present equilibrium $E_1 = (S_p^*, I_{\text{HPV}}^*, I_{cc}^*)$ of the model is locally asymptotically stable if $R_0 > 1$ and unstable if $R_0 < 1$.*

Proof. The cancer present equilibrium $E_1 = (S_p^*, I_{\text{HPV}}^*, I_{cc}^*)$ is locally asymptotically stable (LAS) if all the eigenvalues $\lambda_i, i = 1, 2, 3$, satisfy $\lambda_i < 0$ and $|\arg(\lambda_i)| > \frac{\alpha\pi}{2}$. We present the Jacobean matrix at $E_1 = (S_p^*, I_{\text{HPV}}^* I_{cc}^*)$ for the eigenvalues as

$$\begin{aligned}
&|J(E_1) - \lambda I| \\
&= \begin{vmatrix} -P_v I_{\text{HPV}}^* - \mu_h - \lambda & -P_v S_p^* & 0 \\ P_v I_{\text{HPV}}^* & P_v S_p^* - P_c & 0 \\ & -\mu_h - \lambda & \\ 0 & P_c & -\mu_h - \lambda \end{vmatrix} \\
&= 0. \qquad (28)
\end{aligned}$$

Here, $\lambda_1 = -\mu_h < 0$,

$$\begin{aligned}
|J(E_1) - \lambda I| &= \begin{vmatrix} -P_v I_{\text{HPV}}^* & -P_v S_p^* \\ -\mu_h - \lambda & \\ P_v I_{\text{HPV}}^* & P_v S_p^* - P_c \\ & -\mu_h - \lambda \end{vmatrix} \\
&= 0 \qquad (29) \\
&= \lambda^2 + \lambda(P_v I_{\text{HPV}}^* + 2\mu_h \\
&\quad + P_c - P_v S_p^*) \\
&\quad + (P_v I_{\text{HPV}}^*(P_c + \mu_h) \\
&\quad + \mu_h(P_c + \mu_h) - P_v S_p^* \mu_h) \\
&= 0. \qquad (30)
\end{aligned}$$

The Routh–Hurwitz Criterion of second-order polynomial gives $(P_v I_{\text{HPV}}^* + 2\mu_h + P_c - P_v S_p^*) > 0$ and $(P_v I_{\text{HPV}}^*(P_c + \mu_h) + \mu_h(P_c + \mu_h) - P_v S_p^* \mu_h) > 0$, if $R_o > 1$.

Hence, by Routh–Hurwitz criteria, E_1 is locally asymptotically stable. □

5.1. R_0 Sensitivity Analysis

To test the sensitivity of the reproduction number for each of its parameters

$$\begin{aligned}
A_{P_v} &= \frac{\frac{\partial R_0}{R_0}}{\frac{\partial P_v}{P_v}} = \frac{P_v}{R_0}\frac{\partial R_0}{P_v} = \frac{P_v}{R_0}\left(\frac{1}{P_c + \mu_h}\right) \\
&= \frac{P_v}{P_v}\left(\frac{P_c + \mu_h}{P_c + \mu_h}\right) = 1 > 0. \qquad (31)
\end{aligned}$$

Thus, for example, a 2% increase in P_v would result in a 2% increase in R_0.

$$\begin{aligned}
A_{P_c} &= \frac{\frac{\partial R_0}{R_0}}{\frac{\partial P_c}{P_c}} = \frac{P_c}{R_0}\frac{\partial R_0}{P_c} \\
&= -\frac{P_c}{R_0}\left(\frac{P_v}{(P_c + \mu_h)^2}\right) < 0, \qquad (32)
\end{aligned}$$

and

$$\begin{aligned}
A_{\mu_h} &= \frac{\frac{\partial R_0}{R_0}}{\frac{\partial P_{\mu_h}}{P_{\mu_h}}} = \frac{\mu_h}{R_0}\frac{\partial R_0}{P_{\mu_h}} \\
&= -\frac{\mu_h}{R_0}\left(\frac{\mu_h}{P_o + \mu_h}\right) < 0. \qquad (33)
\end{aligned}$$

The sensitive parameter of the model is P_v. We conclude that the direct ratio is between P_v and the reproduction number R_0. This means that increase in P_v will eventually increase the reproduction number and vice versa. Also, the rest of the parameters are insensitive like P_c and μ_h. We also conclude that the inverse ratio indicates that the parameters are insensitive to the reproduction number R_0. This means an increase in the parameters will reduce reproduction number and vice versa.

6. NUMERICAL SIMULATION

In this section, we implement the proposed technique on a numerical example to observe the graphical solution of cancer model which is given as

$$\begin{aligned}
&{}^{\text{FFM}}_{a}D_t^{\gamma,\theta} S_p \\
&\quad = \mu_h - (P_v I_{\text{HPV}} + \mu_h) S_p, \qquad (34) \\
&{}^{\text{FFM}}_{a}D_t^{\gamma,\theta} I_{\text{HPV}} \\
&\quad = (P_v S_p - P_c - \mu_h) I_{\text{HPV}}, \qquad (35) \\
&{}^{\text{FFM}}_{a}D_t^{\gamma,\theta} I_{cc} \\
&\quad = P_c I_{\text{HPV}} - \mu_h I_{cc} \qquad (36)
\end{aligned}$$

with the following initial conditions:

$$S_p(0) = 0.09, \qquad (37)$$

$$I_{\text{HPV}}(0) = 0.03, \qquad (38)$$

$$I_{cc}(0) = 0.01. \qquad (39)$$

We present the parametric values involved in the proposed fractal-fractional cancer model for CFE as $\mu_h = 0.1$, $P_v = 0.6$, $P_c = 0.7$ and $\sigma = 0.2$. We select the values of parameters for CEE as $\mu_h = 0.1$, $P_v = 1.6$, $P_c = 0.7$ and $\sigma = 0.2$.

The curved lines in Fig. 1 demonstrate the convergence of the susceptible $S_p(t)$ towards the analytically computed equilibrium position. Furthermore, convergence towards the true CFE point may also be observed from the exact value which is discussed before Sec. 4. The parametric values are selected to maintain the value of $R_0 < 1$. The various values of α are prominent in Fig. 1. Here the curve against greater value of α, which is also closed to 1, is rapidly convergent towards the true value of the equilibrium. The rate of convergence for the other values of α may be compared from the graphs, as furnished in Fig. 1.

Figure 2 shows the graphical behavior of I_{HPV} which represents the infectious numeral of HPV female's populace at various values of α by considering the $\beta = 1$. In this figure, we take the set of values of parameters for CFE point which implies that the reproductive number R_0 is less than one. All the

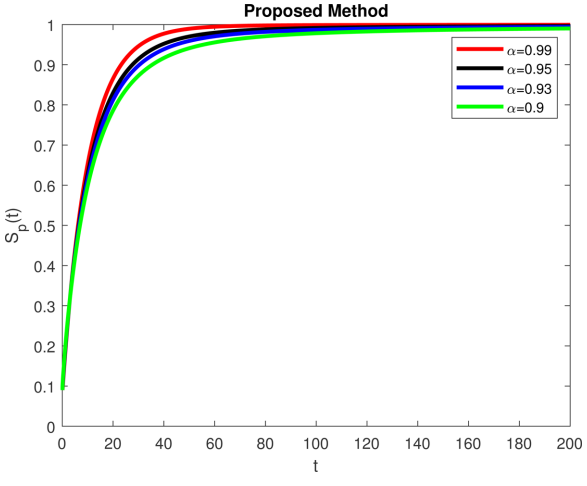

Fig. 1 Numerical simulation for $\beta = 1$.

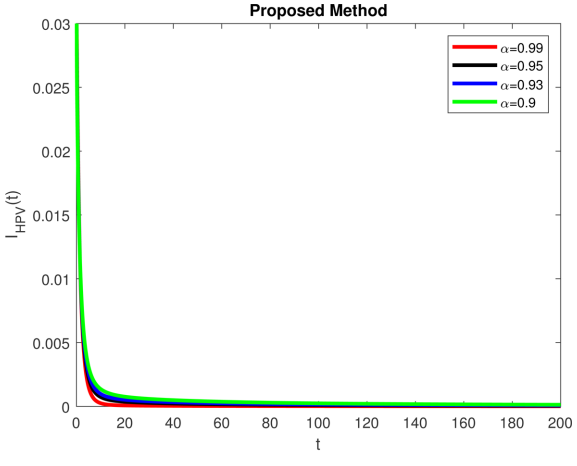

Fig. 2 Numerical simulation for $\beta = 1$.

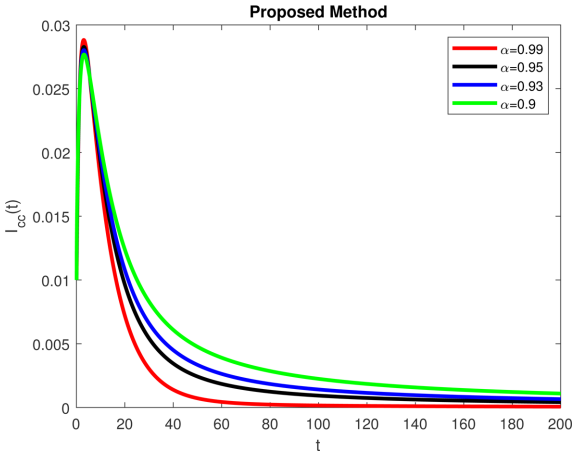

Fig. 3 Numerical simulation for $\beta = 1$.

four curved trajectories in Fig. 3 demonstrate the rate of convergence of women populace with cervical cancer I_{cc} towards the true steady state. It is obvious that the curve converges rapidly towards the equilibrium point when α is closer to 1. The other curves also converge toward the point of equilibrium but their rate is slower as compared to the other curves with greater values of α. For instance, the curve in this figure with $\alpha = 0.9$ has the least rate of convergence towards the equilibrium position.

Figure 4 shows the behavior of three state variables, i.e. $S_p(t)$, $I_{\text{HPV}}(t)$ and $I_{cc}(t)$. All the graphical lines in this figure are drawn at CFE point with certain value of α. The black line describes the susceptible populace of the women community while the other lines represent the infected populace suffering from HPV virus and cervical cancer, respectively. The graphs witness that the number of susceptible

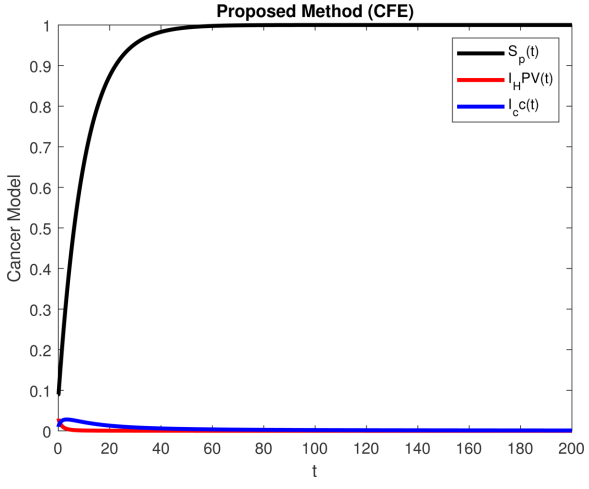

Fig. 4 Numerical simulation for $\beta = 1$ and $\alpha = 1$ for CFE point.

women, i.e. $S_p(t)$ and other categories differentiated in the model touch the disease free equilibrium, with the passage of time. It is also evident from Fig. 4 that the number of infected populace, i.e. $I_{\mathrm{HPV}}(t)$ and $I_{cc}(t)$, approaches zero as time grows, on the other hand, the whole population become susceptible at that stage. This conclusion is in accordance with the biological phenomenon. The sketches in Fig. 5 draw a clear picture of CEE, i.e. when infection exists in the community under study. The susceptible population is not equal to the total population under discussion. But, the sum of all the populations is equal to the total considered population. When the disease persists in the society, there are certain number of infected populace of both types and the susceptible individuals. The graphical values of state variables are same as the exact values calculated in Sec. 4 at CEE.

The curved trajectories in Figs. 6–8 describe the convergence of susceptible $S_p(t)$, populace infected with HPV $I_{\mathrm{HPV}}(t)$ and persons infected with cervical cancer $I_{cc}(t)$. The parametric values are selected in a way that makes $R_0 < 1$ to attain the endemic equilibrium. All the curves in Figs. 6–8 attain the endemic value against different values of α. The curves adopt the different trajectories in the beginning, but ultimately converge to the same value i.e. endemic value. The change in trajectory for the different values of α reflects the change that occurs in the physical phenomenon. So, the role of α in disease dynamics is very important. The values of α also decide how the infection will propagate graphically. On the basis of these sketches, we can interpret the course of disease before reaching the stable position. One important thing is that all the curves converge towards the true steady state,

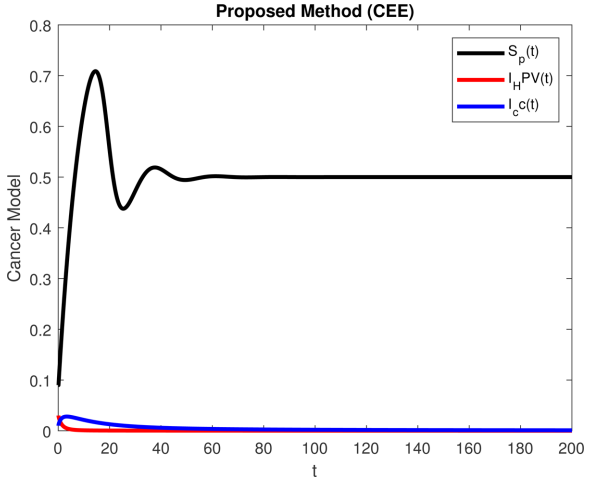

Fig. 5 Numerical simulation for $\beta = 1$ and $\alpha = 1$ for CEE point.

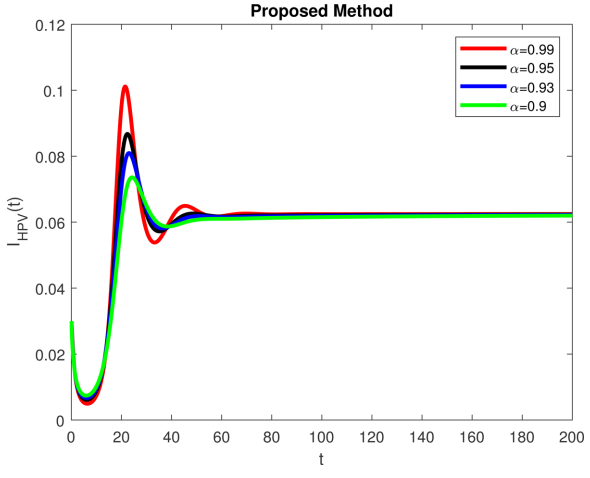

Fig. 7 Numerical simulation for $\beta = 1$.

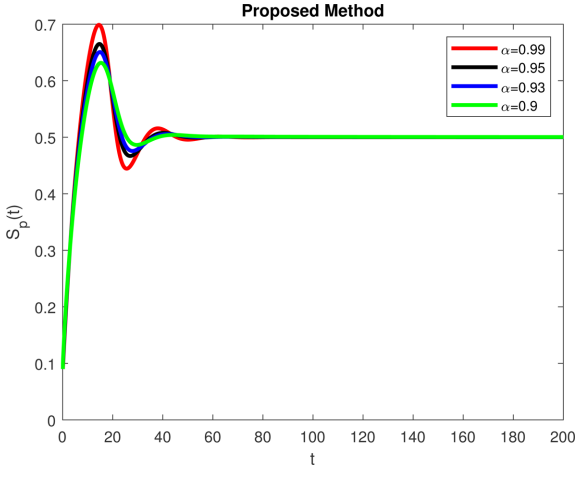

Fig. 6 Numerical simulation for $\beta = 1$.

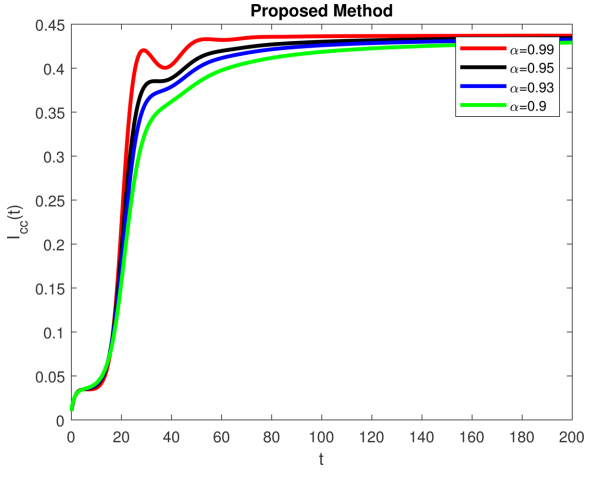

Fig. 8 Numerical simulation for $\beta = 1$.

which strengthens the efficacy and numerical efficiency of the proposed scheme. This fact enhances the worth of the scheme.

Figures 9–11 represent $S(t)$, I_{HPV} and $I_{cc}(t)$, respectively, at CFE. All the graphs in these figures are sketched against $\beta = 0.95$ and the various values of α can be observed from the relevant figure and graph. It has been observed that a change in the value of β affects the path and rate of convergence of the curved graph but the sketch attains the desired position. This fact is very helpful for the modeling of real-world phenomenon. This situation is quite favorable for our proposed numerical fashion. So, by choosing the appropriate values of α and β, we can study the disease dynamics with a more deeper understanding.

Similarly, the graphical patterns in Figs. 12–14 are drawn at CEE. The value of β is chosen as 0.95

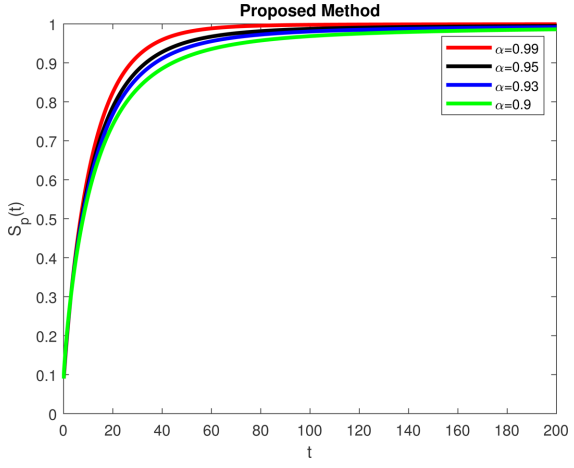

Fig. 9 Numerical simulation for $\beta = 0.95$. and various values of α.

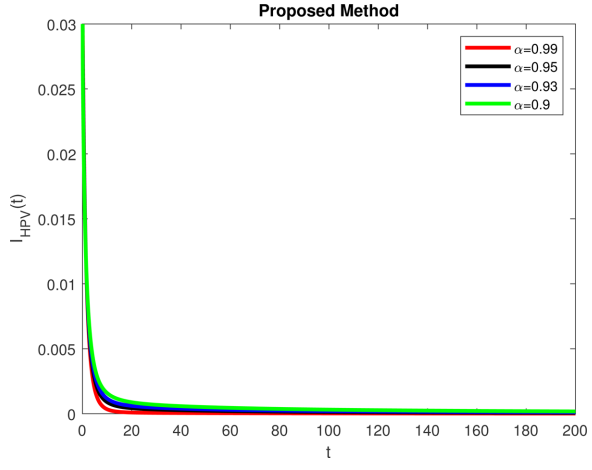

Fig. 10 Numerical simulation for $\beta = 0.95$. and various values of α.

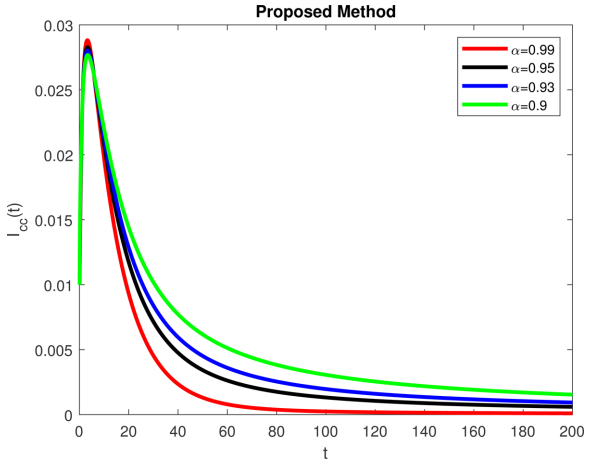

Fig. 11 Numerical simulation for $\beta = 0.95$. and various values of α.

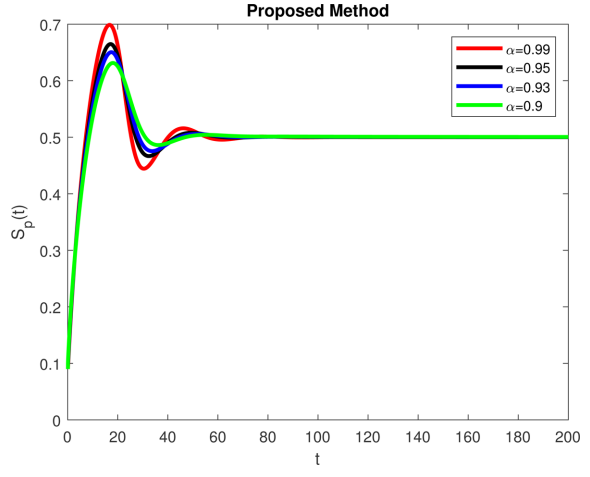

Fig. 12 Numerical simulation for $\beta = 0.95$. and various values of α.

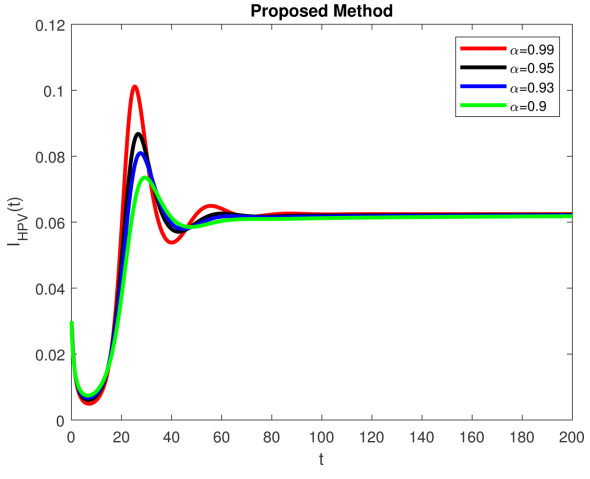

Fig. 13 Numerical simulation for $\beta = 0.95$. and various values of α.

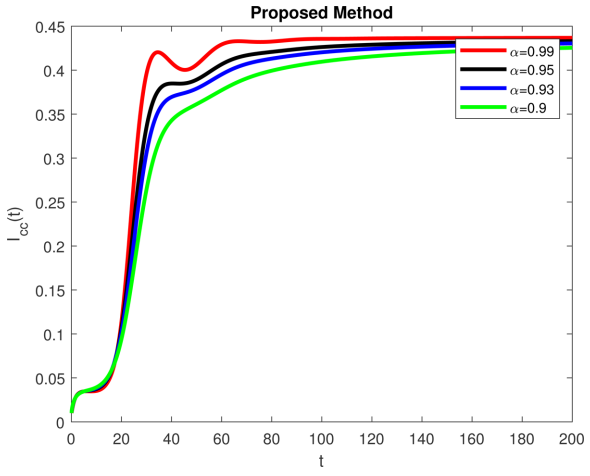

Fig. 14 Numerical simulation for $\beta = 0.95$. and various values of α.

and the values of α are mentioned in each figure. Every graph in each figure converges to the genuine endemic equilibrium as mentioned in Sec. 4. Furthermore, the trajectories against $\beta = 1$ to $\beta = 0.95$ (for a certain values of α) show the slight variation in its route which is due to change in the rate of convergence for both the curved sketches. Also, these sketches reflect the different states of the disease dynamics against certain values of parameters.

So, we can discuss the disease dynamics in various environmental conditions by dint of these graphical templates.

7. CONCLUSION

In this study, an extended fractal fractional model for the malevolent cervical cancer infection caused by HPV is proposed for discussing the transmission and persistence of the disease in the community. A new scheme is designed to investigate the model numerically. The points of equilibria are calculated analytically and verified successfully by numerical simulations. The local stability of the model is investigated and the criteria for the stability are also described at the disease free and endemic equilibrium. These criteria are also tested by simulations. The basic reproduction number R_0 is calculated. Moreover, its role in deciding the stability of the steady state is investigated. Also, the existence and non-existence of the disease in the society is also concluded by R_0. This study may be applied to extend the classical models of the various physical phenomenon for better and vivid perception of the phenomenon. The graphical results of the scheme obtained by the computer simulations are in good agreement with the analytical results. It is also mentionable that all the graphical solutions against different values of α and β converge towards the exact steady states which reflect the worthiness and efficiency of the proposed numerical design. Therefore, this is a reliable scheme to solve the nonlinear models.

For future perspective, the proposed scheme can be applied efficiently on extended fractal fractional predator–prey models, chemical reaction models, etc. Also, the proposed idea can be extended to the reaction-diffusion models.

REFERENCES

1. https: // en.wikipedia.org / wiki / Cervical - cancer - Causes.
2. S. Chakraborty, X. Cao, S. Bhattyacharya and P. K. Roy, The role of HPV on cervical cancer with several functional response: A control based comparative study, *Comput. Math. Modeling* **30**(4) (2019) 1–19.
3. P. Pongsumpun, Mathematical model of cervical cancer due to human papillomavirus infection, *Mathematical Methods in Science and Engineering* (2014), ISBN:978-1-61804-256-9.
4. D. C. A. Taylor, V. Pawar, D. Kruzikas, K. E. Gilmore, A. Pandya, R. Iskandar and M. C. Weinstein, Methods of model calibration observations from a mathematical model of cervical cancer, *Pharmacoeconomics* **28**(11) (2010) 995–1000.
5. F. Khattak, M. Haseeb, S. Fazal, A. Bhatti and M. Ullah, Mathematical modeling of E6-p53 interactions in cervical cancer, *Asian Pac. J. Cancer Prev.* (2017), doi:10.22034/APJCP. 2017.18.4.1057.
6. L. W. K. Bitok, G. P. Pokhariyal, G. McDonnell and R. Abdul, A mathematical model of cervical cancer in Kenya, *Int. J. Sci. Res.* **4**(2) (2015) 1–20.
7. L. S. Lee and A. M. Tameru, A mathematical model of human papillomavirus (HPV) in the United States and its impact on cervical cancer, *J. Cancer* **3** (2012) 262–268.
8. H. L. Peng, S. Tam, L. Xu, K. R. Dahlstrom, C. F. Wu, S. Fu, C. Zhong, W. Chan, E. M. Sturgis, L. Ramondetta, L. Rong, D. R. Lairson and H. Miao, Age-structured population modeling of HPV-related cervical cancer in Texas and US, *Sci. Rep.* **8**(1) (2018) 1–12.
9. A. E. Sado, Mathematical modeling of cervical cancer with HPV transmission and vaccination, *Sci. J. Appl. Math. Statist.* **7**(2) (2019) 21–25.
10. T. S. N. Asih, S. Lenhart, S. Wise, L. Aryati, F. A. Kusumo, M. S. Hardianti and J. Forde, The dynamics of HPV infection and cervical cancer cells, *Bull. Math. Biol.* **78**(1) (2016) 4–20.

11. D. Lestari and R. D. Ambarwati, A local stability of mathematical models for cancer treatment by using gene therapy, *Int. J. Model. Optim.* **5**(3) (2015) 202–219.
12. M. S. A. Mazlan, N. Rosli, N. S. Azmi and A. Bahar, Modeling the cervical cancer growth process by stochastic delay differential equations, *Sains Malaysiana* **44**(8) (2015) 1153–1157.
13. R. V. Barnabas, P. Laukkanen, P. Koskela, O. Kontula, M. Lehtinen and G. P. Garnett, Epidemiology of HPV 16 and cervical cancer in finland and the potential impact of vaccination: Mathematical modeling analyses, *PLOS Med.* **3**(5) (2006) 138–148.
14. S. J. Goldie, M. Diaz, S. Y. Kim, C. E. Levin, H. V. Minh and J. J. Kim, Mathematical models of cervical cancer prevention in the Asia Pacific Region, *J. Vaccine* **26** (2008) 17–29.
15. S. Peprah, F. C. Curreiro, J. H. Hayes, K. Stern, S. Parekh and G. D. Souza, A spatiotemporal analysis of invasive cervical cancer incidence in the state of Maryland between 2003 and 2012, *Cancer Causes Control* **29** (2018) 445–453.
16. C. Xia, C. Ding, R. Zheng, S. Zhang, H. Zeng, J. Wang, Y. Liao, N. Zhang, Z. Yang and W. Chen, Trends in geographical disparities for cervical cancer mortality in China from 1973 to 2013: A subnational spatio-temporal study, *Chin. J. Cancer Res.* **29**(6) (2017) 487–495.
17. E. J. Dasbach, E. H. Elbasha and R. P. Insinga, Mathematical models for predicting the epidemiologic and economic impact of vaccination against human papillomavirus infection and disease, *Epidemiol. Rev.* **28** (2006) 88–100.
18. J. Zhao, S. Virani and H. Sriplung, Spatiotemporal mapping of cervical cancer incidence highlights need for targeted prevention in Songkhla province, Thailand, *Health Policy Plann.* **32** (2017) 430–436.
19. S. J. Goldie, M. Diaz, D. Constenla, N. Alvis, J. K. Andrus and S. Y. Kim, Mathematical models of cervical cancer prevention in Latin America and the Caribbean, *Vaccine* **26** (2008) 59–72.
20. C. Herrmann, S. Ess, B. Thürlimann, N. Hensch and P. Vounatsou, 40 years of progress in female cancer death risk: A Bayesian spatio-temporal mapping analysis in Switzerland, *BMC Cancer* **15**(1) (2015) 666–676.
21. N. Muñoz, X. Castellsagué, A. B. de González and L. Gissmann, Chapter 1: HPV in the etiology of human cancer, *Vaccine* **24**(Suppl. 3) (2006) S3/1–S3/10, doi:10.1016/j.vaccine.2006.05.115.
22. A. Akgül, A novel method for a fractional derivative with non-local and non-singular kernel, *Chaos Solitons Fractals* **114** (2018) 478–482.
23. E. K. Akgül, Solutions of the linear and nonlinear differential equations within the generalized fractional derivatives, *Chaos* **29** (2019) 023108.
24. A. Atangana, Fractal-fractional differentiation and integration: Connecting fractal calculus and fractional calculus to predict complex, system, *Chaos Solitons Fractals* **102** (2017) 396–406.
25. M. Toufik and A. Atangana, New numerical approximation of fractional derivative withnon-local and non-singular kernel: Application to chaotic models, *Eur. Phys. J. Plus* **132** (2017) 444.
26. D. Baleanu, A. Fernandez and A. Akgül, On a fractional operator combining proportional and classical differintegrals, *Mathematics* **8** (2020) 360, doi:10.3390/math8030360.
27. A. Atangana and D. Baleanu, New fractional derivatives with non-local and non-singular kernel, theory and application to heat transfer model, *Thermal Sci.* **20**(2) (2016) 763–769.
28. K. M. Owolabi, A. Atangana and A. Akgül, Modeling and analysis of fractal-fractional partial differential equations: Application to reaction-diffusion model, *Alex. Eng. J.* **59** (2020) 2477–2490.
29. A. Atangana, A. Akgül and K. M. Owolabi, Analysis of fractal fractional differential equations, *Alex. Eng. J.* **59** (2020) 1117–1134.
30. A. Atangana and A. Akgül, Can transfer function and Bode diagram be obtained from Sumudu transform, *Alex. Eng. J.* **59** (2020) 1971–1984.
31. K. A. Abro, Role of fractal-fractional derivative on ferromagnetic fluid via fractal laplace transform: A first problem via fractal-fractional differential operator, *Eur. J. Mech. B Fluids* (2020), doi:10.1016/j.euromechflu.2020.09.002.
32. K. A. Abro and A. Atangana, Numerical study and chaotic analysis of meminductor and memcapacitor through Fractal–Fractional differential operator, *Arab. J. Sci. Eng.* (2020) 1–15 (in press).
33. K. A. Abro, I. Khan and K. S. Nisar, Use of Atangana–Baleanu fractional derivative in helical flow of a circular pipe, *Fractals* **28** (2020) 2040049.